QTAIM Study of Strong H-Bonds with the O−H···A Fragment (A = O, N) in Three-Dimensional Periodical Crystals

M. V. Vener,* A. V. Manaev, A. N. Egorova, and V. G. Tsirelson

Department of Quantum Chemistry, Mendeleev University of Chemical Technology, Miusskaya Square 9, Moscow 125047, Russia

Received: October 27, 2006; In Final Form: December 11, 2006

The relationship between the d(H···A) distance (A = O, N) and the topological properties at the H···A bond critical point of 37 strong (short) hydrogen bonds occurring in 26 molecular crystals are analyzed using the quantum theory of atoms in molecules (QTAIM). Ground-state wave functions of the three-dimensional periodical structures representing the accurate experimental geometries calculated at the B3LYP/6-31G** level of approximation were used to obtain the QTAIM electron density characteristics. The use of an electron-correlated method allowed us to reach the quantitatively correct values of electron density ρ_b at the H···A bond critical point. However, quite significant differences can appear for small absolute values of the Laplacian (<0.5 au). The difference between the H···O and H···N interactions is described using the ρ_b versus d(H···A) dependence. It is demonstrated that the values of parameters in this dependence are defined by the nature of the heavy atom forming the H···A bond. An intermediate (or transit) region separating the shared and closed-shell interactions is observed for the H-bonded crystals in which the bridging proton can move from one heavy atom to another. The crystalline environment changes the location of the bridging proton in strong H-bonded systems; however, the d(O−H)/d(H···O) ratio is approximately the same for both the gas-phase complexes and molecular crystals with a linear or near-linear O−H···O bond.

Introduction

According to Bader's quantum theory of atoms in molecules (QTAIM),[1] the chemical bonds in both isolated species and molecular crystals can be classified and quantified in terms of features of the bond critical points in the electron density, both theoretically and experimentally. The variety of the atomic interactions can be approximately divided into the shared (or covalent) interactions, the intermediate (partially covalent) interactions, and closed-shell (van der Waals, ionic, metal, etc.) interactions.[2−12] The fundamental difference between the two limiting extremes in the interactions, i.e., the closed-shell interactions and shared ones, is the electron density features at the bond critical point. They are the value of electron density, ρ_b, and the sign of the Laplacian of electron density, $\nabla^2\rho_b$, as well as the energy density $h_{e,b} = g_b + \upsilon_b$, where υ_b and g_b are the potential and kinetic energy densities, respectively.[1,13] The shared interactions exhibit $\rho_b \geq 0.14$ au, $\nabla^2\rho_b < 0$, and $h_{e,b} < 0$, while the closed-shell interactions show $\rho_b \leq 0.05$ au, $\nabla^2\rho_b > 0$, and $h_{e,b} > 0$.[1,14] In the intermediate (or transit) region $\nabla^2\rho_b > 0$ and $h_{e,b} < 0$.

An important aspect of the QTAIM application consists of the development of the models, which correlate ρ_b and the bond distance.[2] In particular, Espinosa et al.[8] applied the QTAIM to the study of hydrogen bonds (H-bonds) in the gas-phase X−H···F−Y complexes and revealed the correspondence between the H···F distance and the specific bonding regime. They demonstrated that consideration of the dimensionless $|\upsilon_b|/g_b$ ratio as a function of the H···F distance is useful for the quantification of the atomic interactions within the intermediate region,[8] where $1 < |\upsilon_b|/g_b < 2$.

Classification of the H-bonds as weak, moderate, strong, and very strong ones is based on the correlations of different geometrical and spectroscopic properties of the X−H···A fragment with the distance between the heavy atoms X···A forming the H-bond. These correlations were established for molecular crystals[15,16] and are widely used for correlations of different experimental properties of H-bonded crystals[11,17−24] or computed characteristics of the gas-phase complexes (models) presenting H-bonds of different strength.[25−28] These correlations often do not hold for strong (short) H-bonds having interaction energies in the range of ∼15−40 kcal/mol[29] partly due to mobility of the bridging proton caused by the shape of a potential along the proton coordinate[30−39] and coupling of the proton motion to some low-frequency modes.[40,41] A crystalline environment may change strongly the geometry of H-bonded systems as well as the potential energy surface of the X−H···A fragment.[36,37,42−45] As a result, completely different forms of the strong H-bond potentials in molecular crystals are possible, e.g., see refs 46−49.

Electron density features of the gas-phase complexes with the strong H-bonds were studied in several works.[6−8,10,12,28,50,51] However, no systematic (either experimental or theoretical) QTAIM studies of molecular crystals with strong H-bonds have been published yet. Only a limited number of experimental charge-density analyses for a few molecular crystals with strong H-bonds in the O−H···O fragment are available.[23,30,52−59] A large number of the earlier considered molecular crystals[3,60] exhibit d(H···O) > 1.65 Å, i.e., correspond to the moderate and weak H-bonds. This is why several important problems have not been solved so far; in particular, neither was the difference in the electron density parameters describing the H···O and H···N interactions in molecular crystals characterized quantitatively[7,11] nor was the change in the strong H-bond characteristics due to effects of the crystalline environment considered.

10.1021/jp067057d CCC: $37.00
Published on Web 01/25/2007

The aim of the present study is threefold: (i) we aim to perform the QTAIM study of a set of strong H-bonded molecular crystals that provides statistically significant correlations of the bond critical point properties of the O−H···O fragment (ρ_b, $\nabla^2\rho_b$, $h_{e,b}$, and $|v_b|/g_b$) with the O−H/H···O and O···O distances; (ii) we intend to investigate carefully the region around the point were $\nabla^2\rho_b = 0$ in crystals with strong H-bonds in order to reveal the quantitative difference between the H···O and H···N interactions; (iii) we also purpose to reach the quantitative description of the crystalline environment effects on the geometrical structure and topological electron density properties of the O−H···O fragment by comparison of the computed features of the gas-phase complexes presenting the strong H-bonds with their molecular crystal counterparts. The essential feature of our approach consists of consideration of the equilibrium gas-phase complexes and the use of the electron density computed for the three-dimensional periodical crystals.

Computational Details

The experimentally derived structures of the three-dimensional (3D) periodical crystals under consideration were obtained from the literature; corresponding references will be given in the next section. Periodical electronic wave functions were computed by the CRYSTAL98[61] program at the B3LYP/6-31G** level of approximation. The basis sets for Li^+, Na^+, and K^+ ions were 6-11G, 8-5-11G, and 8-6-5-11G, respectively.[62,63] The QTAIM analysis of the crystalline electron density was performed by the TOPOND computer program.[64]

The structures of the gas-phase complexes with strong H-bonds were optimized at the B3LYP/6-31G** level of approximation with the PC version[65] of the GAMESS(US) program package.[66] The minimum-energy state of all the optimized complexes has been confirmed by calculation of the harmonic frequencies. Topological electron density properties were evaluated by the AIMPAC computer program suite.[67] The equilibrium geometries and wave functions of several gas-phase complexes were also recalculated at the MP2/6-311++G(d,p) level of approximation; this allowed us to be sure that we reached a satisfactory description of the topological electron density properties of the gas-phase complexes with strong and moderate H-bonds.[68]

Results

In the present study, we considered the molecular crystals for which the atomic structures derived by the neutron or high-resolution X-ray diffraction methods are available. We limited ourselves to the normal (or "two center") H-bonds in which the donor X:H interacts with an acceptor :A. The so-called "bifurcated" and "trifurcated" H-bonds[69] as well as the new multiform unconventional H-bonds[70] are beyond the scope of the present study. We did not also consider the crystals with strongly nonlinear fragments, like β-dicarbonyl compounds, which often exhibit a large scattering of the points in structure−property correlations, e.g., see ref 22.

Topological Electron Density Properties of the O−H···O Fragment in the 3D Periodical Crystals. We selected for our study molecular crystals with linear or near-linear O−H···O fragments (−O−H···O > 160°). The unit cells of these compounds contained up to 130 atoms; it allowed one to perform the calculations in the moderately large basis set like 6-31G**.

The ρ_b values in the 3D periodical crystals of urea−phosphoric acid (d(H···O) = 1.259 Å, D(O···O) = 2.41 Å) and KHC_2O_4 computed at the B3LYP/6-31G** level of approximation are in good agreement with the experimentally derived electron density values (Table 1); the relative difference in these quantities is less than 10%. This confirms that the B3LYP/6-31G** level of approximation is suitable for study of the ρ_b values in 3D periodical crystals with strong H-bonds. Agreement between the experimental and computed values of the Laplacian is also reasonable; at the same time, a quite significant difference is observed for small absolute values of $|\nabla^2\rho_b| < 0.5$ au (Table 1). This difference partially originates from the restricted ability of the multiple model to describe the experimental (X-ray diffraction) electron density Laplacian for the bonds having a covalent component.[71]

Relatively large values of ρ_b (≥ 0.13 au), the negative values of the Laplacian, and values of $|v_b|/g_b > 2$ indicate that the H···O interactions in several crystals, such as imidazolium, potassium H maleate, $H_5O_2^+ClO_4^-$, and quinolinic acid, have a significant covalent component. The O−H···O fragment in these crystals is characterized by the following geometrical parameters: D(O···O) ≤ 2.45 Å, d(O−H) ≤ 1.10 Å, and d(H···O) ≤ 1.35 Å; these values are typical for the so-called very short (or very strong) H-bonds. According to Table 1, the Laplacian changes its sign at d(H···O) ≈ 1.35 Å, i.e., it is reasonably close to the extrapolated value of 1.33 Å predicted in ref 3.

In the other 3D periodical crystals, small positive values of the Laplacian, $0.13 < \rho_b < 0.05$ au, and the energy-density characteristics $2 > |v_b|/g_b > 1$ and $-0.1 < h_{e,b} < 0$ au are observed. They indicate all together that the H···O interactions in these crystals can be treated as intermediate-type interactions. The value of $|v_b|/g_b = 1$ was suggested[8,14,89] to define the boundary of the closed-shell interactions. According to our results (Table 1), it is located at D(O···O) ≈ 2.6 Å, d(O−H) ≈ 1.0 Å, and d(H···O) ≈ 1.65 Å. These distances are often considered as a boundary between the strong and moderate H-bonds.[16,19,69,90] It should be noted that the H···O distance corresponding to $|v_b|/g_b = 1$ was already estimated to d(H···O) = 1.64 Å in ref 91.

Thus, the intermediate region separating the ideal shared and closed-shell interactions in crystals with the O−H···O fragment is characterized by the following geometrical parameter ranges: 2.45 ≤ D(O···O) ≤ 2.6 Å, 1.35 Å ≤ d(H···O) ≤ 1.65 Å, and 1.0 Å ≤ d(O−H) ≤ 1.10 Å. For many crystals with these O···O distances, the neutron diffraction reveals the existence of two proton positions separated by distance from 0.1 to 0.7 Å.[92] This phenomenon is usually explained in terms of a double-minimum potential energy surface with a first vibration level of the bridging proton below the central barrier.[33,45,93] Mobility of the bridging proton on such surfaces can be presented as

$$\text{O}-\text{H}\cdots\text{O} \leftrightarrow \text{O}\cdots\text{H}-\text{O}$$

As a result of the proton shift from one heavy atom to another, the hydrogen H···O bond (intermediate type of the atomic interactions) switches to the covalent H−O bond (the shared interactions) and vice versa. This is why the effective structure of the O−H···O fragment in molecular crystals with strong (short) H-bonds may be considered as a superposition of two structures with the bridging proton near the left or right heavy atom. Thus, the intermediate region mainly can be associated with the H-bonded systems in which the bridging proton can move from one heavy atom to another.

The set of the considered molecular crystals enables one to investigate the smooth continuity of the ρ_b dependence on the interaction distance d of a given pair of atoms simultaneously for O−H and H···O bonds.[6,94] It is well-known that electron

TABLE 1: Topological Electron Density Properties at the Bond Critical Points of the O−H···O Fragment Computed Using the Experimental Structures of the 3D Periodical Crystals[a]

H-bonded system (reference for the geometry source)	contact	distance Å	ρ_b au	$\nabla^2\rho_b$ au	$h_{e,b}$ au	$\lvert v_b\rvert/g_b$
imidazolium H maleate (ref 72)	O−H	1.195	0.181	−0.449	−0.207	4.37
	H···O	1.203	0.177	−0.420	−0.199	3.12
quinolinic acid (ref 73)	O−H	1.163	0.197	−0.593	−0.242	3.59
	H···O	1.238	0.160	−0.270	−0.160	3.73
LiH phthalate monohydrate (ref 74)	O−H	1.195	0.179	−0.454	−0.206	3.23
	H···O	1.205	0.174	−0.410	−0.195	3.11
UPA (ref 30), D(O···O) = 2.41 Å[b]	O−H	1.159	0.194 (0.178)	−0.612 (−0.702)	−0.238	3.8
	H···O	1.259	0.143 (0.151)	−0.175 (−0.402)	−0.130	2.51
potassium H maleate (ref 46)	O−H/H···O	1.215	0.171	−0.404	−0.188	3.16
$H_5O_2^+ClO_4^-$ [c]	O−H	1.161	0.191	−0.59	−0.232	3.75
	H···O	1.265	0.144	−0.204	−0.132	2.63
$KH(HCOO)_2$ (ref 76)	O−H	1.165	0.195	−0.610	−0.239	3.76
	H···O	1.270	0.145	−0.188	−0.13	2.56
$KHO(CH_2COO)_2$ (ref 77)	O−H	1.151	0.202	−0.703	−0.255	4.22
	H···O	1.328	0.123	−0.0553	−0.0867	2.18
NaH maleate·$3H_2O$ (ref 78)	O−H	1.079	0.251	−1.05	−0.489	4.99
	H···O	1.367	0.111	0.063	−0.062	1.81
2,3,5,6-pyrazinetetracarboxylic acid dihydrate (ref 79)	O−H	1.072	0.250	−1.107	−0.277	4.53
	H···O	1.411	0.0964	0.0986	−0.041	1.63
picolinic acid *N*-oxide (ref 80)	O−H	1.04	0.282	−1.322	−0.423	5.56
	H···O	1.424	0.100	0.122	−0.0418	1.58
KHC_2O_4 (ref 58)	O−H	1.06	0.264 (0.28)	−1.23 (−1.16)	−0.385	5.96
	H···O	1.457	0.085 (0.080)	0.129 (0.077)	−0.027	1.45
monomethylammonium H oxalate (ref 81)	O−H	1.032	0.284	−1.445	−0.440	6.58
	H···O	1.486	0.0784	0.148	−0.0192	1.34
α-oxalic acid (ref 82)	O−H	1.026	0.285	−1.470	−0.446	6.65
	H···O	1.478	0.0806	0.142	−0.022	1.38
$NaHC_2O_4$ H_2O (ref 83)	O−H	1.036	0.281	−1.432	−0.430	6.94
	H···O	1.531	0.0694	0.141	−0.0129	1.27
PDA (ref 31), 15 K[d]	O−H	1.025	0.291	−1.553	−0.459	7.52
	H···O	1.558	0.0625	0.149	−0.008	1.18
dimethylammonium H oxalate (ref 84)	O−H	0.988	0.321	−1.90	−0.558	7.72
	H···O	1.545	0.0675	0.156	−0.0104	1.21
L-glutamic acid (ref 85)	O−H	1.024	0.295	−1.56	−0.463	7.34
	H···O	1.568	0.0634	0.145	−0.0085	1.19
$KHCO_3$ (ref 86)	O−H	1.005	0.311	−1.737	−0.511	7.66
	H···O	1.587	0.0606	0.149	−0.0062	1.14
UPA (ref 30), D(O···O) = 2.589 Å	O−H	1.005	0.302	−1.68	−0.493	7.73
	H···O	1.585	0.0583	0.150	−0.061	1.14
PDA (ref 31), 296 K	O−H	1.004	0.310	−1.776	−0.514	8.32
	H···O	1.608	0.0541	0.148	−0.0032	1.08
L-tyrosine (ref 87)	O−H	1.018	0.302	−1.646	−0.480	8.00
	H···O	1.610	0.0555	0.143	−0.004	1.10
L-glutamic acid HCl (ref 88)	O−H	1.017	0.303	−1.671	−0.484	8.33
	H···O	1.624	0.0506	0.144	−0.0014	1.04
UPA (ref 30), D(O···O) = 2.649 Å	O−H	1.000	0.31	−1.77	−0.515	8.11
	H···O	1.642	0.0516	0.137	−0.0037	1.09

[a] Experimental values of ρ_b and $\nabla^2\rho_b$ are given in parentheses. [b] Urea−phosphoric acid; the three H-bonds with different O···O distances exist in this crystal (ref 30). [c] Positions of the H atoms in the$H_5O_2^+ClO_4^-$ crystal are not available (ref 75); therefore, the computed geometry (ref 36) was used instead. [d] Pyridine-3,5-dicarboxylic acid.

density at the bond critical points varies exponentially with interaction distance.[6,7,10,11,28] For the sake of simplicity, this nonlinear regression function is replaced by its logarithmic version[6,7]

$$\ln \rho_b = (1.676 \pm 0.017) - (2.840 \pm 0.013)d; \quad R^2 = 0.999, \quad n = 47 \quad (1)$$

In contrast with the work in ref 6, where only the *intermolecular* strong H-bonds were considered, eq 1 spans both *inter*- and *intramolecular* strong H-bonds. Such generality of eq 1 implies that topological electron density peculiarities of H-bonds are practically the same for both inter- and intramolecular interactions, in accord with the observation in ref 10.

To interpret eq 1, it should be noted that the distances in the O−H···O fragment are interrelated (Figure 1). The dependence d(O−H) d (H···O) = constant was discussed elsewhere.[18,69,94] It is caused by the dependence of the both values on the O···O distance, see Figure 2. As the O···O and H···O separations are shortened, the O−H bond length increases. Distances of the two bonds become equal to each other for very short (strong) H-bonds 2.39 ≤ D(O···O) ≤ 2.45 Å. Due to the d(O−H) d

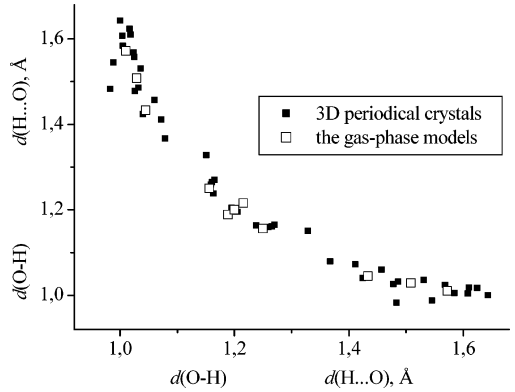

Figure 1. d(O−H) vs d(H···O) distances obtained from the neutron and high-resolution X-ray diffraction crystal structures (black boxes) and computed for the gas-phase models (empty boxes).

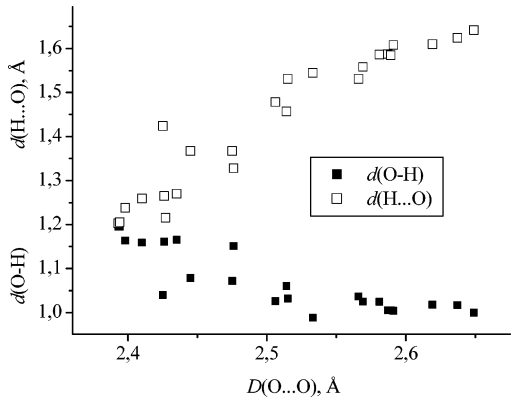

Figure 2. d(O−H)/d(H···O) vs D(O···O) distances in the 3D periodical crystals.

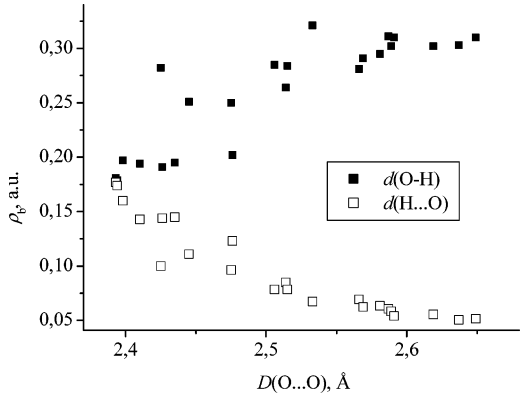

Figure 3. Computed ρ_b values vs D(O···O) distances in the 3D periodical crystals.

(H···O) = constant dependence and the fact that the two distances are going to coincide with each other for the very strong H-bonds, the d(O−H)/d(H···O) separations can be treated simultaneously and used as the "controlling parameter"[95] which defines the electron density properties of the O−H···O fragment in H-bonded crystals. It should be noted that the dependence of ρ_b on the O···O distance is characterized by a strong scattering of the electron density values for D(O···O) ≤ 2.45 Å. Figure 3 illustrates the well-known fact[12,26] that the structure−property correlations often do not hold for very strong H-bonds.

Special attention should be paid to the $|\upsilon_b|/g_b$ values computed for the O−H bond forming the O−H···O fragment (Table 1). We found that it increases monotonously with the O−H distance decrease, i.e., increase d(H···O)·($|\upsilon_b|/g_b$) ≈ 3 for very strong H-bonds (imidazolium and potassium H maleates, $H_5O_2^+ClO_4^-$, etc.), $|\upsilon_b|/g_b \approx 8$ for d(O−H) ≈ 1.0 Å (dimethylammonium H oxalate crystals), while $|\upsilon_b|/g_b \approx 10$ for d(O−H) ≈ 0.991 Å (the O−H groups of the water molecules, involved in moderate H-bonds with the ClO_4^- ions in $H_5O_2^+ClO_4^-$ crystals, see Figure 1 in ref 36). We conclude that the $|\upsilon_b|/g_b$ index, which is a useful tool for defining the intermediate region boundaries, deserves an additional consideration as a descriptor of the covalent O−H bonds involved in H-bonding.

H···O versus H···N Strong H-Bonds: the $\nabla^2\rho_b = 0$ Region. The atomic structures of a set of molecular crystals with strong O−H···N bonds have been studied recently by neutron and high-resolution X-ray diffraction.[31,32,96−98] We used these structural data to perform the electron density calculations for the 3D periodical crystals and to investigate carefully the region around the point $\nabla^2\rho_b = 0$. Computed values of ρ_b, $\nabla^2\rho_b$, $h_{e,b}$, and $|\upsilon_b|/g_b$ are given in Table 2. Special attention should be paid to the pentachlorophenol complex with 4-methylpuridine (4-MePy), which is characterized at very low (20 K) and room temperature by the asymmetric bridge, while at ∼90 K the bridging proton locates approximately at the midpoint between the O and N atoms.[32,34] The O···H and H···N distances at 80−100 K are close to each other; however, their topological electron density properties differ strongly (Table 2). The difference between the O···H and H···N interactions was described by comparison of the parameter values in the $\rho_b = \rho_b(d)$ dependences that were evaluated using Table 2:

$$\ln \rho_b = (1.682 \pm 0.060) - (2.829 \pm 0.048)\, d(\text{O−H/H···O interactions}); \quad R^2 = 0.997, \quad n = 13 \quad (2a)$$

$$\ln \rho_b = (1.611 \pm 0.014) - (2.677 \pm 0.010)\, d(\text{N−H/H···N interactions}); \quad R^2 = 0.999, \quad n = 13 \quad (2b)$$

Particular values of the parameters entering eq 2b are very close to the corresponding ones, 1.640 au and 2.704 $Å^{-1}$, calculated for N−H/H···N interactions in the gas-phase systems with the N−H···O fragment.[28] On the other hand, they differ from those in eq 2a in accord with ref 28. This means that the particular values of the parameters in the $\rho_b = \rho_b(d)$ dependence are defined by the nature of the heavy A atom forming the H···A bond.

According to our computations, the Laplacian changes its sign at d(H···O) ≈ 1.35 Å and d(H···N) ≈ 1.42 Å. Theoretical QTAIM analysis of the gas-phase H-bonded systems with the N−H···O fragment has showed[68] that the point $\nabla^2\rho_b = 0$ falls in the region of 1.34 < d(H···N) < 1.42 Å. This is very close to the value found in the present study dealing with the 3D periodical crystals. The obtained results imply that the value of the H···A distance, at which $\nabla^2\rho_b = 0$, is defined by the nature of the heavy atom A. Indeed, the boundary of the shared interactions for the X−H···F fragment locates at d(H···F) ≈ 1.62 Å.[8] To interpret this observation, one has to consider the dependence of the X−H/H···A distances on the X···A separation, e.g., see Figure 2. The point is that the shortest X···A distance, D_{min}(X···A), is specified by the sort of X and A atoms forming the H-bond: D_{min}(O···O) ∼ 2.39 Å,[21,88,99] D_{min}(N···O) ∼ 2.52 Å ,[34] and D_{min}(F···F) ∼ 2.23 Å.[100] This is why the d values defining the boundaries of the intermediate region are *different* for various heavy atoms forming the X−H···A fragment. According to the present study, this region is placed in the range of 1.35 ≤ d(H···O) ≤ 1.65 Å for the O−H···O fragment, while it is located in the range 1.62 ≤ d(H···F) ≤ 1.96 Å for the X−H···F fragment.[8]

Environmental Influence on Strong H-Bonds: Molecular Crystals versus Gas-Phase Models. Most of the strong

TABLE 2: Topological Electron Density Properties at Critical Points of the N−H···O/N···H−O Fragment Computed Using the Experimental Structure of the 3D Periodical Crystals with the Strong H-Bonds

crystal	O···H/H−O Å	ρ_b au	$\nabla^2\rho_b$ au	$h_{e,b}$ au	$\lvert\nu_b\rvert/g_b$	N−H/H···N Å	ρ_b au	$\nabla^2\rho_b$ au	$h_{e,b}$ au	$\lvert\nu_b\rvert/g_b$
3-MePy[a]	1.440	0.0907	0.123	−0.032	1.51	1.141	0.238	−1.08	−0.321	5.31
BT−BIPy 20 K[b]	1.326	0.127	−0.04	−0.087	2.13	1.206	0.198	−0.720	−0.238	5.11
PDA 15 K[c]	1.311	0.133	−0.081	−0.0996	2.26	1.213	0.195	−0.688	−0.232	4.88
4-MePy 20 K[d]	1.309	0.132	−0.0643	−0.0974	2.20	1.206	0.197	−0.704	−0.236	4.93
4-MePy 80 K	1.266	0.148	−0.202	−0.134	2.61	1.256	0.173	−0.493	−0.183	4.07
4-MePy 100 K	1.258	0.152	−0.232	−0.142	2.69	1.265	0.169	−0.455	−0.173	3.91
4-MePy 125 K	1.241	0.159	−0.300	−0.159	2.89	1.288	0.159	−0.371	−0.151	3.57
4-MePy 200 K	1.229	0.164	−0.349	−0.171	3.05	1.304	0.152	−0.318	−0.138	3.37
PDA 298 K	1.218	0.171	−0.41	−0.187	3.22	1.307	0.151	−0.308	−0.137	3.29
2NIP[e]	1.203	0.186	−0.522	−0.216	3.54	1.325	0.145	−0.208	−0.119	2.78
	1.145	0.216	−0.773	−0.280	4.24	1.383	0.124	−0.0613	−0.0798	2.23
2-MePy[f]	1.068	0.257	−1.132	−0.365	5.51	1.535	0.0821	0.0739	−0.0265	1.59
BT−BIPy 20 K	1.069	0.259	−1.163	−0.369	5.71	1.551	0.0789	0.0771	−0.0237	1.55

[a] 3-Methylpyridine 2,6-dichloro-nitrophenol (ref 96). [b] The 1:2 cocrystal of benzene-1,2,4,5-tetracarboxylic acid and 4,4′-bipyridyl (ref 97). [c] Pyridine-3,5-dicarboxylic acid (ref 31). [d] 4-Methylpyridine-pentachlorophenol (ref 32). [e] 2-(*N*-methyl-α-imioethyl)-phenol (ref 98). [f] 2-Methylpyridine-pentachlorophenol (ref 32).

TABLE 3: Comparison of the O−H···O Fragment Distances Computed for the Gas-Phase Models Presenting the Strong H-Bonds with the Experimental Values in Their Molecular Crystal Counterparts[a]

			gas-phase model[b]				
system	contact	molecular crystal (source for structure)	distance Å	ρ_b au	$\nabla^2\rho_b$ au	$h_{e,b}$ au	$\lvert\nu_b\rvert/g_b$
H phthalate ion	O···O	2.394 (ref 46)	2.378				
$H[C_8H_4O_4]^-$	H···O	1.205	1.189	0.182	−0.453	−0.212	3.16
	O−H	1.195					
$H_5O_2^+$	O···O	2.426[c]	2.396 (2.381)				
	H···O	1.265	1.200 (1.192)	0.168 (0.161)	−0.418 (−0.428)	−0.190 (−0.195)	3.24 (3.22)
	O−H	1.116					
H maleate ion	O···O	2.397 (2.437)[d]	2.406				
$H[C_4H_2O_4]^-$	H···O	1.203 (1.22)	1.250	0.155	−0.234	−0.150	2.65
	O−H	1.195 (1.22)	1.156	0.201	−0.626	−0.250	3.66
$[H(HCOO)_2]^-$	O···O	2.437 (ref 76)	2.428				
	H···O	1.270	1.215	0.167	−0.394	−0.184	3.16
	O−H	1.165					
quinolinic acid	O···O	2.398 (ref 73)	2.476				
$C_7H_5NO_4$	H···O	1.238	1.433	0.092	0.136	−0.033	1.51
	O−H	1.163	1.045	0.277	−1.329	−0.416	6.01
urea−phosphoric acid	O···O	2.41 (ref 30)	2.536				
$(NH_2)_2CO/PO(OH)_3$	H···O	1.259	1.509	0.071	0.157	−0.013	1.25
	O−H	1.160	1.029	0.283	−1.454	−0.439	6.78
picolinic acid *N*-oxide	O···O	2.425 (ref 80)	2.513 (2.515)				
$C_6H_5NO_3$	H···O	1.42	1.572 (1.572)	0.067 (0.063)	0.167 (0.181)	−0.009 (−0.013)	1.18 (1.24)
	O−H	1.04	1.010 (1.001)	0.314 (0.316)	−1.715 (−2.320)	−0.507 (−0.639)	7.49 (11.83)

[a] The values of ρ_b, $\nabla^2\rho_b$, $h_{e,b}$, and $\lvert\nu_b\rvert/g_b$ at the O−H/H···O bond critical points, computed for the gas-phase models, are also given. [b] The distances and ρ_b, $\nabla^2\rho_b$, $h_{e,b}$, and $\lvert\nu_b\rvert/g_b$ values, computed using the MP2/6-311++G(d,p) level, are given in parentheses. [c] See footnote *a* to Table 1. [d] Imidazolium H maleate (ref 72); the data for KH maleate are given in the parentheses (ref 46).

H-bonded systems listed in Table 1 cannot be observed in the gas-phase. Some of them (such as $KHO(CH_2COO)_2$ and mono- and dimethylammonium H oxalates, KHC_2O_4) form polymeric chains or planar sheets (pyridine-3,5-dicarboxylic acid) in the crystal phase, of which naturally no analogues exist in the gas phase. The strong intermolecular H-bond in 2,3,5,6-pyrazine-tetracarboxylic acid dihydrate crystals is broken in the gas phase. Charged H-bonded dimers, e.g., $(HCO_3)_2^{2-}$ in $KHCO_3$, can indeed be associated with the gas-phase dimers under some limitations,[58,101,102] which however make problematic a direct comparison with their molecular crystal counterparts. Zwitter-ions (such as the molecular crystals of L-glutamic acid and L-tyrosine) are usually nonstable in the gas phase. The H maleate and H phthalate ions, $H_5O_2^+$, quinolinic and urea−phosphoric acids, $KH(HCOO)_2$, and picolinic acid *N*-oxide can exist as the gas-phase systems. No experimental investigations of these systems in the gas phase have been published yet. To our knowledge, the $H_5O_2^+$ ion is the only gas-phase system with a very strong H-bond and near-linear O−H···O fragment whose IR spectrum was measured in the different frequency regions.[103,104] This is why the *computed* geometries of the gas-phase models with strong H-bonds are compared with the *experimental structures* of their molecular crystal counterparts in Table 3. The H-bonded systems in molecular crystals given in the Table 3 represent three different classes of strong H-bonds:[105] negative charge-assisted (potassium hydrogen di-formate, H maleate, and H phthalate ions), positive charge-assisted ($H_5O_2^+$), and resonance-assisted (quinolinic and urea−phosphoric acids, picolinic acid *N*-oxide).

In accord with the early reported data,[36,48] the crystalline environment practically does not change the O···O distance in the charge-assisted H-bonds (Table 3). The situation is different

in the case of the resonance-assisted H-bonds. The O···O distances computed for the gas-phase models of picolinic acid *N*-oxide[106] and urea−phosphoric acid[37] are found to be much longer than the values in their molecular crystal counterparts (Table 3). The present results for quinolinic acid support this observation. Table 3 shows that the crystalline environment strongly changes the location of the bridging proton in the considered models of the resonance-assisted and charge-assisted H-bonds. The point is that the d(O−H)/d(H···O) relationship established for *molecular crystals* with strong H-bonds is also valid for the *gas-phase models*, see Figure 1.

According to Table 3, the geometrical parameters of the O−H···O fragment and electron density at the O−H/H···O bond critical points computed for the $H_5O_2^+$ ion and picolinic acid *N*-oxide using B3LYP/6-31G** are close to the corresponding values obtained using the MP2/6-311++G(d,p) level of approximation. This supports the use of the B3LYP/6-31G** method for computation of the electron density in the O−H/H···O bond critical points for the gas-phase models employed in Table 3. These values were added to the set of ρ_b values calculated for the 3D periodical crystals (Tables 1 and 2), and the logarithmic regression function ln ρ_b versus d for *all* O−H/H···O bonds, considered in the present study, was recalculated:

$$\ln \rho_b = (1.673 \pm 0.018) - (2.834 \pm 0.014)d; \quad R^2 = 0.998, \quad n = 71 \quad (3)$$

Comparison of the parameter values entering eq 3 and eq 1 shows that topological features of the O−H···O fragment in the gas-phase models and the 3D periodical crystals are described by the *same* $\rho_b(d)$ dependence. This observation suggests that the computed QTAIM properties of the gas-phase H-bonded complexes may be used for interpretation of the experimental electron densities of their molecular counterparts.[56]

According to Table 3, the $\nabla^2\rho_b$, $h_{e,b}$, and $|v_b|/g_b$ values computed using the MP2/6-311++G(d,p) level of approximation can differ from the B3LYP/6-31G** values. In particular, quite significant differences in the $\nabla^2\rho_b$ and $|v_b|/g_b$ values appear for the covalent O−H bond in picolinic acid *N*-oxide. This implies that the B3LYP/6-31G** level of approximation should be used with caution for general QTAIM discussions involving H-bond features either in 3D periodical crystals or in the gas phase.

Discussion

A unique exponential dependence has been used to fit the computed ρ_b values coming from both intra- and intermolecular interactions (eqs 1, 2a, and 3). This contrasts with the analysis carried out by other authors, pointing to the occurrence of two different exponential dependences for those interactions.[8] To clarify this problem, a log−linear plot for the 3D periodical crystals and gas-phase models is given in Figure 4. One can see that intra- and intermolecular H-bonds do fit a unique line. This is possible due to consideration of the *near-linear* intramolecular O−H···O fragments (−O−H···O > 160°), most of which occur in seven-membered pseudocycles. A large number of intramolecular O−H···A (A = O, N) bonds occur in six-membered pseudocycles and are strongly nonlinear.[11,23,28,53−57] This set of strong H-bonded systems requires the use of a special exponential dependence.

We demonstrated that the H···A distance corresponding to the boundaries of the intermediate region is defined by the nature of the A atom. This means that the particular values of the parameters in the $\rho_b = \rho_b(d)$ dependence are different for

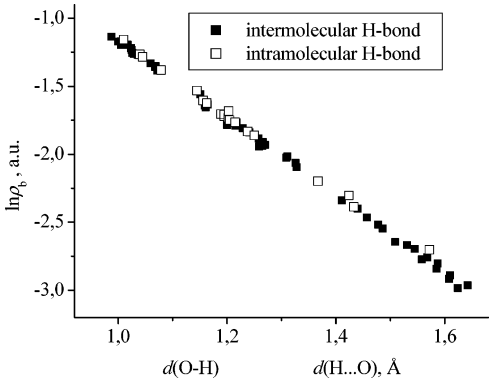

Figure 4. Computed ln ρ_b values vs the d(O−H)/d(H···O) distances for the intermolecular (black boxes) and intramolecular (empty boxes) H-bonds.

different heavy atoms forming the H···A fragment, cf., eqs 2a and 2b. This difference may be negligible for the moderate and weak H-bonds; however, it is significant for the strong and very strong H-bonds. To illustrate this statement, consider the values of the parameters entering eq 3 as evaluated in refs 6 and 10. According to ref 6, they equal 1.29 au and 2.51 Å^{-1} for the gas-phase complexes with strong intermolecular H-bonds and the X−H···O fragment X = C, F, Cl. These values differ from the corresponding ones, 1.04 au and 2.394 Å^{-1}, estimated from the available experimental ρ_b values for molecular crystals with the X−H···O fragment.[5] In the case of the X−H···A fragment, where X = O, N, F, C and A = O, N, F, theoretical values were 2.61 au and 2.38 Å^{-1}; see ref 10. Summing up, the exponential dependence of electron density at the bond critical point for the H···A interaction can be considered as a universal one. However, the particular values of the parameters in this dependence are defined by the nature of the heavy atom forming the H···A bond.

To conclude, we like to note that Espinosa and Molins[91] developed an approach that enables one to retrieve the atomic interaction potentials from the topology of electron density for moderate and weak H-bonds (d(H···O) > 1.65 Å) which belong to the pure closed-shell interactions. Unfortunately, this approach is of limited applicability for strong H-bonded systems because an account for the partial covalent character of the interaction is needed. In addition, the H-bond potential energy surface is, at least, two-dimensional in the latter case, e.g., see refs 19, 35, 41, and 43. A model *two-dimensional* potential of the quasi-symmetric O−H···O fragment in the molecular crystals was developed some time ago[92] and was successfully applied for interpretation of spectroscopic[90,107] and dynamic[108] peculiarities of strong H-bonded systems in condensed phases. The problem of retrieving two-dimensional potential energy surfaces in molecular crystals with strong H-bonds in the O−H···N fragment is a challenging task. It has not been solved yet; corresponding work is in progress now.

Conclusions

An intermediate (transit) region separating the shared and closed-shell interactions is observed for H-bonded crystals in which the bridging proton can move from one heavy atom to another. In the case of the O−H···O fragment this region is characterized by the following geometrical parameter ranges: 2.45 ≤ D(O···O) ≤ 2.6 Å, 1.35 ≤ d(H···O) ≤ 1.65 Å, and 1.0 ≤ d(O−H) ≤ 1.10 Å.

Exponential dependence of the electron density at the bond critical point on the H···A (A = O, N) distance can be

considered as a "universal" one. The particular values of the parameters in this dependence are defined by the nature of the heavy atom forming the H···A bond. According to our computations, the value of the H···A distance, at which $\nabla^2\rho_b = 0$, equals ~1.35 Å for H···O and ~1.42 Å for H···N.

The crystalline environment changes the location of the bridging proton in strong H-bonded systems; however, the d(O−H)/d(H···O) ratio is approximately the *same* in the gas-phase complexes and their molecular crystal counterparts with linear or near-linear O−H···O bonds (−O−H···O > 160°).

Acknowledgment. This study was supported by the Russian Federal Agency for Education (Program "Development of the Highest-School Scientific Potential: 2006−2008", Project 2.1.1.5051) and the Russian Foundation for Basic Research, Grant 07-03-00702. We thank Professor C. Gatti for making the TOPOND software available for us. M.V.V. thanks Professor Dusan Hadzi for useful comments and Drs. A. I. Stash and K. A. Lyssenko for help in the numerical calculations.

References and Notes

(1) Bader, R. F. W. *Atoms in Molecules. A Quantum Theory*; Oxford University Press: New York, 1990.
(2) Alkorta, I.; Barrrios, L.; Rozas, I.; Elguero, J. *J. Mol. Struct.* (*THEOCHEM*) **2000**, *496*, 131.
(3) Espinosa, E.; Molins, E.; Lecomte, C. *Chem. Phys. Lett.* **1998**, *285*, 170.
(4) Spackman, M. A. *Chem. Phys. Lett.* **1999**, *301*, 425.
(5) Espinosa, E.; Souhassou, M.; Lachekar, H.; Lecomte, C. *Acta Crystallogr., Sect. B* **1999**, *55*, 563.
(6) Alkorta, I.; Elguero, J. *J. Phys. Chem. A* **1999**, *103*, 272.
(7) Knop, O.; Rankin, K. N.; Boyd, R. J. *J. Phys. Chem. A* **2001**, *105*, 6552.
(8) Espinosa, E.; Alkorta, I.; Elguero, J.; Molins, E. *J. Chem. Phys.* **2002**, *117*, 5529.
(9) Ranganathan, A.; Kulkarni, G. U.; Rao, C. N. R. *J. Phys. Chem. A* **2003**, *107*, 6073.
(10) Tang, T.-H.; Deretey, E.; Jensen, S. J. K.; Csizmadia, I. G. *Eur. Phys. J. D* **2006**, *37*, 217.
(11) Dominiak, P. M.; Makal, A.; Mallinson, P. R.; Trzcinska, K.; Eilmes, J.; Grech, E.; Chruszcz, M.; Minor, W.; Woźniak, K. *Chem. Eur. J.* **2006**, *12*, 13564.
(12) Grabowski, S. J.; Sokalski, W. A.; Dyguda, E.; Leszczyński, J. *J. Phys. Chem. B* **2006**, *110*, 6444.
(13) Tsirelson, V. G.; Ozerov, R. P. *Electron Density and Bonding in Crystals*; Institute of Physics Publishing: Bristol and Philadelphia, 1996.
(14) Tsirelson, V. G. *Acta Crystallogr., Sect. A* **1999**, *55*, Suppl. Abstract M13-OF-003.
(15) Hamilton, W. C.; Ibers, J. A. *Hydrogen Bonding in Solids*; Benjamin: New York, 1968.
(16) Novak, A. *Struct. Bonding* **1974**, *18*, 177.
(17) Ferraris, G.; Franchini-Angela, M. *Acta Crystallogr., Sect. B* **1972**, *28*, 3572.
(18) Olovsson, I.; Jönsson, P.-G. In *The Hydrogen Bond. Recent Developments in Theory and Experiments*; Schuster, P., Zundel, G., Sandorfy, C., Eds.; North Holland Publishing Co.: Amsterdam, 1976; Vol. 2.
(19) Sokolov, N. D.; Savel'ev, V. A. *Chem. Phys.* **1977**, *22*, 383.
(20) Howard, J.; Tomkinson, J.; Eckert, J.; Goldstone, J. A.; Taylor, A. D. *J. Chem. Phys.* **1983**, *78*, 3150.
(21) Ichikawa, M. *Acta Crystallogr., Sect. B* **1978**, *34*, 2074.
(22) Steiner, T.; Saeger, W. *Acta Crystallogr., Sect. B* **1994**, *50*, 348.
(23) Gilli, P.; Bertolasi, V.; Ferretti, V.; Gilli, G. *J. Am. Chem. Soc.* **2000**, *122*, 10405.
(24) Sobczyk, L.; Grabowski, S. J.; Krygowski, T. M. *Chem. Rev.* **2005**, *105*, 3513.
(25) Scheiner, S. *J. Am. Chem. Soc.* **1981**, *103*, 315.
(26) Kumar, G. A.; McAllister, M. A. *J. Am. Chem. Soc.* **1998**, *120*, 3159.
(27) Parthasarathi, R.; Subramanian, V.; Sathyamurthy, N. *J. Phys. Chem. A* **2006**, *110*, 3349.
(28) Grabowski, S. J.; Małecka, M. *J. Phys. Chem. A* **2006**, *110*, 11847.
(29) Jeffrey, J. A. *An Introduction to Hydrogen Bonding*; Oxford University Press: Oxford, 1997.
(30) Rodriges, B. L.; Tellgren, L.; Fernandes, N. G. *Acta Crystallogr., Sect. B* **2001**, *57*, 353.
(31) Cowan, J. A.; Howard, J. A. K.; McIntyre, G. J.; Lo, S. M.-F.; Williams, I. D. *Acta Crystallogr., Sect. B* **2003**, *59*, 794.
(32) Steiner, T.; Majerz, I.; Wilson, C. C. *Angew. Chem., Int. Ed.* **2001**, *40*, 2651.
(33) Kreevoy, M. M.; Marimanikkuppam, S.; Young, V. G.; Baran, J.; Szafran, M.; Schultz, A. J.; Trouw, F. *Ber. Bunsen-Ges. Phys. Chem.* **1998**, *102*, 370.
(34) Sobczyk, L. *Ber. Bunsen-Ges. Phys. Chem.* **1998**, *102*, 377.
(35) Basilevsky, M. V.; Vener, M. V. *Usp. Khim.* **2003**, *72*, 3; *Russ. Chem. Rev.* **2003**, *72*, 1.
(36) Vener, M. V.; Sauer, J. *Phys. Chem. Chem. Phys.* **2005**, *7*, 258.
(37) Morrison, C. A.; Siddick, M. M.; Camp, P. J.; Wilson, C. C. *J. Am. Chem. Soc.* **2005**, *127*, 4042.
(38) Fontaine-Vive, F.; Johnson, M. R.; Kearley, G. J.; Cowan, J. A.; Howard, J. A. K.; Parker, S. F. *J. Chem. Phys.* **2006**, *124*, 234503.
(39) Perrin, C. L.; Nielson, J. B. *Annu. Rev. Phys. Chem.* **1997**, *48*, 511.
(40) Sekiya, H.; Nagashima, Y.; Nishimura, Y. *J. Chem. Phys.* **1990**, *92*, 5761.
(41) Herek, J. L.; Pedersen, S.; Banares, L.; Zewail, A. H. *J. Chem. Phys.* **1992**, *97*, 9046.
(42) Firth, D. W.; Barbara, P. F.; Trommsdorff, H. P. *Chem. Phys.* **1989**, *136*, 349.
(43) Meyer, R.; Ernst, R. R. *J. Chem. Phys.* **1990**, *93*, 5518.
(44) Fillaux, F.; Lautié, A.; Tomkinson, J.; Kearley, G. J. *Chem. Phys.* **1991**, *154*, 135.
(45) Vener M. V. In *Hydrogen-Transfer Reactions. Handbook/Reference Book*; Hynes, J. T., Klinman, J. P., Limbach, H.-H., Schowen, R. L. , Eds.; Wiley-VCH: Weinheim, Germany, 2006; p 273.
(46) Fillaux, F.; Leygue, N.; Tomkinson, J.; Cousson, A.; Paulus, W. *Chem. Phys.* **1999**, *244*, 387.
(47) Fillaux, F.; Cousson, A.; Tomkinson, J. *Chem. Phys. Lett.* **2004**, *399*, 289.
(48) Wilson, C. C.; Thomas, L. H.; Morrison, C. A. *Chem. Phys. Lett.* **2003**, *381*, 102.
(49) Wilson, C. C.; Thomas, L. H.; Morrison, C. A. *Chem. Phys. Lett.* **2004**, *399*, 292.
(50) Ziólkowski, M.; Grabowski, S. J.; Leszczyński, J. *J. Phys. Chem. A* **2006**, *110*, 6514.
(51) Pacios, L. F. *J. Phys. Chem. A* **2004**, *108*, 1177.
(52) Flensburg, C.; Larsen, S.; Stewart, S. F. *J. Phys. Chem.* **1995**, *99*, 10130.
(53) Madsen, D.; Flensburg, C.; Larsen, S. *J. Phys. Chem. A* **1998**, *102*, 2177.
(54) Madsen, G. K. H.; Iversen, B. B.; Larsen, F. K.; Kapon, M.; Reisner, J. M.; Herbstein, F. H. *J. Am. Chem. Soc.* **1998**, *120*, 10040.
(55) Madsen, G. K. H.; Wilson, C.; Nymand, T. M.; McIntyre, M. J.; Larsen, F. K. *J. Phys. Chem. A* **1999**, *103*, 8684.
(56) Gilli, P.; Bertolasi, V.; Pretto, L.; Lyčka, A.; Gilli, G. *J. Am. Chem. Soc.* **2002**, *124*, 13554.
(57) Mallinson, P. R.; Smith, G. T.; Wilson, C. C.; Grech, E.; Wozniak, K. *J. Am. Chem. Soc.* **2003**, *125*, 4259.
(58) Macchi, P.; Iversen, B. B.; Sironi, A.; Chakoumakos, B. C.; Larsen, F. K. *Angew. Chem., Int. Ed.* **2000**, *39*, 2719.
(59) Scheins, S.; Dittrich, B.; Messerschmidt, M.; Paulmann, C.; Luger, P. *Acta Crystallogr., Sect. B* **2004**, *60*, 184.
(60) Flaig, R.; Koritsanszky, T.; Dittrich, D.; Wagner, A.; Luger, P. *J. Am. Chem. Soc.* **2002**, *124*, 3407.
(61) Saunders, V. R.; Dovesi, R.; Roetti, C.; Causa, M.; Harrison, N. M.; Orlando, R.; Zikovich-Wilson, C. M. *CRYSTAL 98 User's Manual*; Universita di Torino: Torino, Italy, 1998.
(62) Ojamäe, L.; Hermannson, K.; Pisani, C.; Causa, M.; Roetti, K. *Acta Crystallogr., Sect. B* **1994**, *50*, 268.
(63) Prencipe, M.; Zupan, A.; Dovesi, R.; Apra, E.; Saunders, V. R. *Phys. Rev. B* **1995**, *51*, 3391.
(64) Gatti, C. *TOPOND98 User's Manual*; CNR-CSRSRC: Milano, Italy, 1999.
(65) Granovsky, A. A. *PC GAMESS*, version 7.0, http://classic-.chem.msu.su/gran/gamess/index.html.
(66) Schmidt, M. W.; Baldridge, K. K.; Boatz, J. A.; Elbert, S. T.; Gordon, M. S.; Jensen, J. H.; Koseki, S.; Matsunaga, N.; Nguyen, F. A.; Su, S.; Windus, T. L.; Dupuis, M.; Montgomery, J. A. *J. Comput. Chem.* **1993**, *14*, 1347.
(67) Bieger-Konig, W. F.; Bader, R. F. W.; Tang, T. H. *J. Comput. Chem.* **1982**, *3*, 317.
(68) Grabowski, S. J.; Sokalski, W. A.; Leszczyński, J. *J. Phys. Chem. A* **2006**, *110*, 4772.
(69) Steiner, T. *Angew. Chem., Int. Ed.* **2002**, *41*, 48.
(70) Alkorta, I.; Rozes, I.; Elguero, J. *Chem. Soc. Rev.* **1998**, *27*, 163.
(71) Tsirelson, V. G. In *Recent Advances in Quantum Theory of Atoms in Molecules*; Matta, C., Boyd, R. R., Eds.; Wiley-VCH: Weinheim, Germany, 2007, p 259.
(72) Shu, B.; Schlemper, E. O. *Acta Crystallogr., Sect. B* **1980**, *36*, 3017.

(73) Kvick, Å; Koetzle, T. F.; Thomas, R.; Takusagava, F. *J. Chem. Phys.* **1974**, *60*, 3866.
(74) Kuppers, H.; Takusagava, F.; Koetzle, T. F. *J. Chem. Phys.* **1982**, *85*, 5636.
(75) Olovsson, I. *J. Chem. Phys.* **1968**, *49*, 1063.
(76) Hermannson, K.; Tellgren, R.; Lehmann, M. S. *Acta Crystallogr., Sect. B* **1983**, *39*, 1507.
(77) Albertsson, J.; Grenthe, I. *Acta Crystallogr., Sect. B* **1973**, *29*, 2751.
(78) Olovsson, G.; Olovsson, I.; Lehmann, M. S. *Acta Crystallogr., Sect. C* **1984**, *40*, 1521.
(79) Vishweshwar, P.; Babu, N. J.; Nangia, A.; Mason, S. A.; Pushmann, H.; Mondal, R.; Howard, J. A. K. *J. Phys. Chem. A* **2004**, *108*, 9406.
(80) Steiner, T.; Schreurs, A. M. M.; Lutz, M.; Kroon, J. *Acta Crystallogr., Sect. C* **2000**, *56*, 577.
(81) Thomas, J. O. *Acta Crystallogr., Sect. B* **1975**, *31*, 2156.
(82) Sabine, T. M.; Cox, G. W.; Craven, B. M. *Acta Crystallogr., Sect. B* **1969**, *25*, 2437.
(83) Delaplane, R. G.; Tellgren, R.; Olovsson, I. *Acta Crystallogr., Sect. B* **1984**, *40*, 1800.
(84) Thomas, J. O.; Pramatus, S. *Acta Crystallogr., Sect. B* **1975**, *31*, 2159.
(85) Lehmann, M. S.; Nunes, A. C. *Acta Crystallogr., Sect. B* **1980**, *36*, 1621.
(86) Thomas, J. O.; Tellgren, R.; Olovsson, I. *Acta Crystallogr., Sect. B* **1974**, *30*, 2540.
(87) Frey, M. N.; Koetzle, T. F.; Lehmann, M. S.; Hamilton, W. C. *J. Chem. Phys*. **1973**, *58*, 2547.
(88) Sequeira, A.; Hajagopal, H.; Chidambaram, R. *Acta Crystallogr., Sect. B* **1972**, *28*, 2514.
(89) Gatti, C. *Z. Kristallogr.* **2005**, *220*, 399.
(90) Sokolov, N. D.; Vener, M. V.; Savel'ev, V. A. *J. Mol. Struct.* **1990**, *222*, 365.
(91) Espinosa, E.; Molins, E. *J. Chem. Phys.* **2000**, *113*, 5686.
(92) Sokolov, N. D.; Vener, M. V.; Savel'ev, V. A. *J. Mol. Struct.* **1988**, *177*, 93.
(93) Belot, J. A.; Clark, J.; Cowan, J. A.; Harbison, J. S.; Kolesnikov, A. I.; Kye, Y-S.; Schultz, A. J.; Silvenrnail, K.; Zhao, X. *J. Phys. Chem. B* **2004**, *108*, 6922.
(94) Bürgi, H. B.; Dunitz, J. D. *Acc. Chem. Res.* **1983**, *16*, 153.
(95) Costales, A.; Blanco, M. A.; Pendas, A. M.; Mori-Sanchez, P.; Luana, V. *J. Phys. Chem. A* **2004**, *108*, 2794.
(96) Majerz, I.; Sawka-Dobrowolska, W.; Sobczyk, L. *J. Mol. Struct.* **1993**, *297*, 177.
(97) Cowan, J. A.; Howard, J. A. K.; McIntyre, G. J.; Lo, S. M.-F.; Williams, I. D. *Acta Crystallogr., Sect. B* **2003**, *59*, 794.
(98) Filarowski, A.; Gloviaka, T.; Koll, A. *J. Mol. Struct.* **1999**, *484*, 75.
(99) Joswig, W.; Fuess, H.; Ferraris, G. *Acta Crystallogr., Sect. B* **1982**, *38*, 2798.
(100) Catti, M.; Ferraris, G. *Acta Crystallogr., Sect. B* **1976**, *32*, 2754.
(101) Bean, J.; Chen, Z. *J. Phys. Chem. A* **1997**, *101*, 3526.
(102) Braga, D.; D'Oria, E.; Grepioni, F.; Mota, F.; Novoa, J. J.; Rovira, C. *Chem. Eur. J.* **2002**, *8*, 1173.
(103) Yeh, L. I.; Okumura, M.; Myers, J. D.; Price, J. M.; Lee, Y. T. *J. Chem. Phys.* **1989**, *91*, 7319.
(104) Asmis, K. R.; Pivonka, N. L.; Santambrogio, G.; Brümmer, M.; Kaposta, C.; Neumark, D. M.; Wöste, L. *Science* **2003**, *299*, 1375.
(105) Gilli, G.; Gilli, P. *J. Mol. Struct.* **2000**, *552*, 1.
(106) Panek, J.; Stare, J.; Hadzi, D. *J. Phys. Chem. A* **2004**, *108*, 7417.
(107) Vener, M. V. *Chem. Phys.* **1992**, *166*, 311.
(108) Sakun, V. P.; Vener, M. V.; Sokolov, N. D. *J. Chem. Phys.* **1996**, *105*, 379.